



Brazilian Journal of Physics

ISSN: 0103-9733

luizno.bjp@gmail.com

Sociedade Brasileira de Física

Brasil

Mushtaq, A.; Shah, AttaUllah; Ikram, M.; H. Clark, R. E.  
Sheared Flow Driven Drift Instability and Vortices in Dusty Plasmas with Opposite Polarity  
Brazilian Journal of Physics, vol. 46, núm. 1, febrero, 2016, pp. 78-86  
Sociedade Brasileira de Física  
São Paulo, Brasil

Available in: <http://www.redalyc.org/articulo.oa?id=46443233010>

- How to cite
- Complete issue
- More information about this article
- Journal's homepage in redalyc.org


redalyc.org

Scientific Information System

Network of Scientific Journals from Latin America, the Caribbean, Spain and Portugal

Non-profit academic project, developed under the open access initiative

# Sheared Flow Driven Drift Instability and Vortices in Dusty Plasmas with Opposite Polarity

A. Mushtaq<sup>1</sup> · AttaUllah Shah<sup>2</sup> · M. Ikram<sup>3</sup>  · R. E. H. Clark<sup>4</sup>

Received: 1 September 2015 / Published online: 5 November 2015  
© Sociedade Brasileira de Física 2015

**Abstract** Low-frequency electrostatic drift waves are studied in an inhomogeneous dust magnetoplasma containing dust with components of opposite polarity. The drift waves are driven by the magnetic-field-aligned (parallel) sheared flows in the presence of electrons and ions. Due to sheared flow in the linear regime, the electrostatic dust drift waves become unstable. The conditions of mode instability, with the effects of dust streaming and opposite polarity, are studied. These are excited modes which gain large amplitudes and exhibit interactions among themselves. The interaction is governed by the Hasegawa-Mima (HM) nonlinear equation with vector nonlinearity. The stationary solutions of the HM equation in the form of a vortex chain and a dipolar vortex, including effects of dust polarity and electron (ion) temperatures, are studied. The relevance of the present work to space and laboratory four component dusty plasmas is noted.

**Keywords** Four component dust plasma · Kelvin-Helmholtz instability · Electrostatic drift waves · Hasegawa Mima equation · Drift vortices

## 1 Introduction

Currently, there is a great deal of interest in the physics of dusty plasmas, i.e., plasmas with extremely massive and charged dust grains. Such plasmas occur in laboratory, astrophysical, and space environments such as cometary tails [1, 2], the upper mesosphere [3], Jupiter's magnetosphere [1, 4], etc. The presence of static dust modifies the existing plasma wave spectra [5], while the inclusion of dust charge dynamics results in new eigen modes such as dust acoustic waves [6, 7] and dust-ion-acoustic waves [8, 9]. All of these studies are based on a commonly used dusty plasma model that assumes electrons, ions, and negatively charged dust. The consideration of negatively charged dust is due to the fact that in low-temperature laboratory plasmas, the collection of plasma particles (viz. electrons and ions) is the only important charging process, and the thermal speeds of electrons far exceeds that of ions. However, there can be some other important charging processes by which dust grains become positively charged [10–12]. The principal mechanisms by which dust grains become positively charged are photoemission in the presence of a flux of ultraviolet photons [10], thermionic emission induced by radiative heating [12], secondary emission of electrons from the surface of the dust grains [11], etc. The existence of positively charged dust in various regions of space, such as cometary tails [1, 2], the upper mesosphere [3], and Jupiter's magnetosphere [1, 4], has been observed. There is direct evidence of the coexistence of positively and negatively charged dust in different regions of space, viz. Earth's mesosphere [3], cometary tails [1, 13], Jupiter's magnetosphere [1, 4], dense molecular clouds, etc. Chow et al. [11] have shown theoretically that due to the size effect on secondary emission, insulating dust grains with different sizes can have opposite polarities, the smaller ones

✉ M. Ikram  
mikphysics@gmail.com

<sup>1</sup> Department of Physics, Abdul Wali Khan University, Mardan, 23200, Pakistan

<sup>2</sup> Institute of Physics & Electronics, University of Peshawar, Peshawar, 25000, Pakistan

<sup>3</sup> Department of Physics, Hazara University, 21300 Mansehra, Pakistan

<sup>4</sup> Departments of Physics and Astronomy, University of Texas at San Antonio, San Antonio, TX, USA

being positive and the larger ones being negative. The opposite situation, i.e., larger (massive) ones being positive and smaller (lighter) ones being negative, is also possible by triboelectric charging [14, 15]. This is predicted from the observations of dipolar electric fields perpendicular to the ground with the negative pole at higher altitudes, generated by dust devils [16, 17] and sand storms [18]. The formation of these dipolar electric fields means that negatively charged smaller (i.e., lighter) dust is blown upward in the convection, while positively charged larger (more massive) dust remains at the surface due to gravity. It is shown experimentally, using Mars-like dust in a simulation wind tunnel, that  $\mu$ -sized dust can carry net charges of around  $10^5 e$ , and there can be almost equal quantities of positively and negatively charged dust in the suspension [14, 17]. The coexistence of larger (massive) positively charged dust and smaller (lighter) negatively charged dust [19–21], or with reversed polarity, [22] is also observed in laboratory devices [19–22] where dust of polymer materials is used. It may be noted here that the coexistence of the same sized dust of opposite polarity may also occur by photoemission if the photoemission yields of the dust-material are different [23]. Recently, based on these theoretical predictions and satellite/experimental observations, a number of authors [14, 24–26] have considered a dusty plasma with dust of opposite polarity, and have investigated linear [14] and nonlinear [24–26] electrostatic waves without [14, 24–26] or with an external static magnetic field. Very recently, the solitonic, periodic, and quasiperiodic behaviors of dust acoustic and dust ion acoustic waves with Maxwell-distributed and superthermal ( $q$ -nonextensive and kappa distributed) electrons and ions were studied using bifurcation theory of planar dynamical systems [27–30]. The nonlinear propagation and interaction of dust acoustic multi-solitons in a four component dusty plasma comprised of negatively and positively charged cold dust fluids, non-thermal electrons, and ions were recently investigated with effects of overtaking collision and phase shifts of multi-solitons [31].

Sheared flow has a significant role both in linear and nonlinear electrostatic oscillations in non-uniform magnetoplasmas and has been discussed by several authors [32–35]. Shukla et al. [32] derived the nonlinear propagation of low-frequency electrostatic waves in a strongly magnetized electron–positron plasma in the presence of parallel [32] and perpendicular [33] sheared plasma flows with massive charged dust grains. Sheared flow driven drift waves and the counter-rotating vortices in electron–positron–ion plasmas have also been studied [34]. Laboratory experiments have been carried out that shed light on the role of velocity sheared flow on plasma stability and ion energizing in wave-induced mechanisms [36, 37]. Rocket and satellite observations have predicted the effect of sheared plasma

flow on auroral acceleration and transport processes [38–42]. Collaborations among laboratory, space, and theory research groups have resulted in joint publications on the role of shear flow-driven waves in auroral acceleration and transport phenomena [38, 43, 44].

Parallel-velocity shear refers to an inhomogeneity in the radial profile of magnetic-field-aligned (parallel) drift velocity. Different techniques have been proposed for the production of parallel-velocity shear in a magnetized plasma plane where the electrons and ions are injected from one or both sides [45–47]. These methods utilize one or more injection or termination electrodes, whose bias voltage or work function differ at different radial positions to produce radially inhomogeneous acceleration or retardation of ions in the direction of the applied magnetic field. Perpendicular-velocity shear can be caused by radially non-homogeneous radial electric fields that produce ions and electrons with a radially inhomogeneous  $E \times B$  drift-velocity profile. These radial electric fields have been produced using biased, radially segmented, circular electrode plates either at the electron-injection boundary [48–50] and the electron-termination boundary [51], or at both end boundaries [52].

The aim of current work is to investigate the behavior of the dust drift wave (Kelvin-Helmholtz type) instability arising from sheared flow parallel to the magnetic field in oppositely charged dusty plasmas containing an appreciable fraction of Boltzmann electron and ions. In the presence of sheared flow, the electrostatic modes interact among themselves nonlinearly. The corresponding mode coupling equations are governed by a set of nonlinear equations in which we incorporate the transverse two-dimensional vector nonlinearity due to the polarization drift and nonlinearity due to the coupling between the  $E \times B$  and parallel opposite dusts flow. It is shown that stationary solutions of the nonlinear mode coupling equations can be represented in the form of a vortex street and a dipolar vortex.

## 2 Governing Equations

Consider an inhomogeneous magnetized dusty plasma consisting of cold positively and negatively charged dust, and inertialess electrons and ions. We assume that the negative dust particles are much more massive than positively charged dust particles. This model is similar to the dusty plasmas found in a cometary tail [1, 2], the upper mesosphere [3], and Jupiter's magnetosphere [1, 4]. Let  $n_i$ ,  $n_e$ ,  $n_{d+}$ , and  $n_{d-}$  represent the density of ion, electron, positively charged and the negatively charged dusts, respectively. Let  $m_i$ ,  $m_e$ ,  $m_{d+}$ , and  $m_{d-}$  represent the respective masses while  $T_i$  and  $T_e$  represent the respective temperatures of the

ions and electrons. At equilibrium, we have  $Z_{d+}n_{d+0}(x) + n_{i0}(x) = Z_{d-}n_{d-0}(x) + n_{e0}(x)$ , where  $n_{dj0}(x)$  is the unperturbed nonuniform number density of the  $j$ th dust species ( $j = +$  for positive dust and  $-$  for negative dust). In the presence of an inhomogeneous flow of the  $j$ th species along the magnetic field lines  $\hat{z}V_{dj0}(x)$  having gradients along the  $x$ -axis (sheared flows, which are maintained by external sources, generate a negligibly small sheared magnetic field), for an obliquely propagating perturbation, the plasma may become unstable due to sheared flow instability. This instability may arise because of the fact that adjacent layers of the streaming fluid have different velocities and it develops when the change in the perpendicular velocity exceeds some critical value. The equilibrium sheared flow can be maintained by external forces, such as a body force, a constant electric field, etc. Let the equilibrium magnetic field be  $\mathbf{B}_0 = B_0\hat{z} + B_{0y}(x)\hat{y}$  with assumption that  $B_{0y} \ll B_0$  so that the equilibrium magnetic field should be homogeneous.  $\hat{z}$  and  $\hat{y}$  are the unit vectors along the  $z$  and  $y$  directions respectively. But this  $B_{0y}$  is still the source term for the  $V_{dj0}(x)$  in a self consistent way. Some authors [53] have incorporated the effect of  $B_{0y}$  for a parallel sheared driven instability, and it has been shown that it has very small impact on the dispersion properties of the wave concerned. Therefore, according to the aforementioned assumption, we assume that in the unperturbed state, the dust species are freely streaming along the magnetic field lines with an inhomogeneous velocity  $V_{dj0}(x)$ . This concept has been used by Jovanovic and Shukla [54] for nonlinear inertial-Alfvén structures driven by parallel sheared flows. Thus, owing to the above facts, the motion of the two oppositely charged dust components is described by their continuity and momentum equations,

$$\frac{\partial n_{dj}}{\partial t} + \nabla \cdot (n_{dj}\mathbf{v}_{dj}) = 0, \quad (1)$$

$$\left(\frac{\partial}{\partial t} + \mathbf{v}_{dj} \cdot \nabla\right) \mathbf{v}_{dj} = \frac{q_{dj}}{m_{dj}} (\mathbf{E} + \mathbf{v}_{dj} \times \mathbf{B}_0), \quad (2)$$

where  $\mathbf{v}_{dj} = \mathbf{v}_{dj\perp} + \hat{z}v_{djz} + \hat{y}V_{dj0}(x)$ . The cold dust steady state requires  $E_0 \neq 0$  and  $V_{dj0}(x) = -(1/B_{0y})\frac{\partial\phi_0}{\partial x}$  where  $\phi_0$  is the equilibrium electrostatic potential. The ions and electrons have smaller inertia compared to dust particulates and therefore follow the Boltzmann distribution

$$n_i = n_{i0} \exp\left[-\frac{e\phi}{K_B T_i}\right] \quad (3)$$

$$n_e = n_{e0} \exp\left[\frac{e\phi}{K_B T_e}\right] \quad (4)$$

The above (2) for  $j$ th dust component can be written

$$d_t^j \mathbf{v}_{dj} = -\frac{q_{dj}}{m_{dj}} \nabla\phi \pm \Omega_{cdj} (\mathbf{v}_{dj} \times \hat{\mathbf{z}}), \quad (5)$$

where  $\Omega_{cdj} = \frac{Z_{dj}eB_0}{m_{dj}c}$  is the dust gyrofrequency, and

$d_t^j = \frac{\partial}{\partial t} + \mathbf{v}_E \cdot \nabla_{\perp} + (v_{djz} + V_{dj0}(x))\frac{\partial}{\partial z}$ . In the case of low-frequency perturbations (in comparison with the dust gyrofrequency), the parallel components of opposite dust fluid velocities are described by

$$D_t v_{djz} - \frac{c\dot{V}_{dj0}}{B_0} \partial_y \phi = \frac{Z_{dj}e}{m_{dj}} \partial_z \phi, \quad (6)$$

where  $\dot{V}_{dj0} = \partial_x V_{dj0}$  is the shear flow velocity and  $|D_t| = \left|\partial_t + \frac{c}{B_0} \hat{z} \times \nabla \phi \cdot \nabla\right|$  with the assumption that  $|D_t| \gg (V_{dj0} + v_{djz})\partial_z$  [32]. The perpendicular velocities in a cold plasma can be written as

$$\begin{aligned} \mathbf{v}_{dj\perp} &\approx \frac{c}{B_0} \hat{z} \times \nabla \phi + \frac{Z_{dj}c}{B_0 \Omega_{cdj}} \left(\partial_t + \frac{c}{B_0} \hat{z} \times \nabla \phi \cdot \nabla + (V_{dj0} + v_{djz})\partial_z\right) \nabla_{\perp} \phi \\ &\approx \mathbf{v}_E + \mathbf{v}_{pdj} \end{aligned} \quad (7)$$

where  $\mathbf{v}_E$  is the  $\mathbf{E} \times \mathbf{B}$  drift and  $\mathbf{v}_{pdj}$  is the dust polarization drift. Here,  $\phi$  is the electrostatic potential. The continuity (1) for negatively charged dust is

$$\begin{aligned} D_t Z_{d-} n_{d-} + \mathbf{v}_E \cdot \nabla_{\perp} Z_{d-} n_{d-o} + Z_{d-} n_{d-o} (\nabla_{\perp} \cdot \mathbf{v}_{d-\perp}) \\ + Z_{d-} n_{d-o} \partial_z v_{d-z} = 0, \end{aligned} \quad (8)$$

and, similarly, the corresponding continuity equation for positively charged dust is

$$\begin{aligned} D_t Z_{d+} n_{d+} + \mathbf{v}_E \cdot \nabla_{\perp} Z_{d+} n_{d+o} + Z_{d+} n_{d+o} (\nabla_{\perp} \cdot \mathbf{v}_{d+\perp}) \\ + Z_{d+} n_{d+o} \partial_z v_{d+z} = 0. \end{aligned} \quad (9)$$

Using (7–9), it follows that

$$\begin{aligned} D_t (Z_{d-} n_{d-} - Z_{d+} n_{d+}) + \frac{c}{B_0} (Z_{d+} n_{d+o} + Z_{d-} n_{d-o}) \kappa_{ei} \partial_y \phi \\ = -\frac{c}{B_0} \left(\frac{Z_{d+} n_{d+o}}{\Omega_{cd+}} + \frac{Z_{d-} n_{d-o}}{\Omega_{cd-}}\right) D_t (\nabla_{\perp}^2 \phi) \\ - \partial_z (Z_{d+} n_{d+o} v_{d+z} - Z_{d-} n_{d-o} v_{d-z}) \end{aligned} \quad (10)$$

where the  $\kappa_{ei} = \partial_x (n_{e0} - n_{i0}) / (Z_{d+} n_{d+o} + Z_{d-} n_{d-o})$  is the inverse inhomogeneous scale length and  $\Omega_{cdj} = |Z_{dj}eB_0/m_{dj}c|$  is the dust cyclotron frequency. Using the Poisson's equation

$$\nabla^2 \phi = 4\pi e (Z_{d-} n_{d-} - Z_{d+} n_{d+} + n_e - n_i), \quad (11)$$

with (10) and linearized form of (3–4) we get

$$\begin{aligned} D_t \left[ \nabla^2 + \left(\frac{\omega_{pd+}^2}{\Omega_{cd+}^2} + \frac{\omega_{pd-}^2}{\Omega_{cd-}^2}\right) \nabla_{\perp}^2 - k_D^2 \right] \phi \\ = -\left(\frac{\omega_{pd+}^2}{\Omega_{cd+}^2} + \frac{\omega_{pd-}^2}{\Omega_{cd-}^2}\right) \kappa_{ei} \partial_y \phi - 4\pi e (Z_{d-} n_{d-o} \partial_z v_{d-z} \\ - Z_{d+} n_{d+o} \partial_z v_{d+z}) \end{aligned} \quad (12)$$

Here,  $\omega_{pd_j} = \sqrt{\frac{4\pi(Z_{d_j}e)^2 n_{d_j0}}{m_{d_j}}}$  is the  $j$ th dust plasma frequency and  $k_D = \sqrt{\frac{4\pi e^2 n_{e0}}{k_B T_e} + \frac{4\pi e^2 n_{i0}}{k_B T_i}}$  is the effective inverse Debye Length.

### 3 Linear Dispersion Relations

Equations (6) and (12) are the governing equations for nonlinearly coupled electrostatic waves in a non-uniform opposite dust magnetoplasma containing Boltzmann electrons and ions in the presence of parallel sheared dust flows. In the linear limit, we neglect the nonlinear terms in (6) and (12), assuming that the perturbation is proportional to  $\exp[i(k_y y + k_z z - \omega t)]$ , after some algebraic manipulation we obtain the following dispersion relation

$$\omega^2 \left[ k^2 + k_y^2 \left( \frac{\omega_{pd+}^2}{\Omega_{cd+}^2} + \frac{\omega_{pd-}^2}{\Omega_{cd-}^2} \right) + k_D^2 \right] + \left( \frac{\omega_{pd+}^2}{\Omega_{cd+}^2} + \frac{\omega_{pd-}^2}{\Omega_{cd-}^2} \right) \kappa_{ei} k_y \omega = \left( \omega_{pd+}^2 + \omega_{pd-}^2 \right) k_z^2 + \frac{\omega_{pd+}^2}{\Omega_{cd+}^2} (\delta \dot{V}_{d+o} - \dot{V}_{d+o}) k_y k_z, \quad (13)$$

where  $\delta = \frac{Z_{d-} n_{d-0}}{Z_{d+} n_{d+0}}$ . We have considered Boltzmann electrons and ions in an opposite polarity dusty plasma embedded in an external magnetic field  $B = B_0 \hat{z}$  where  $B_0$  is the strength of the magnetic field and  $\hat{z}$  is a unit vector along the  $z$ -axis. In the presence of low-frequency (in comparison with the dust gyro frequency), the dispersion relation (13) for opposite charge dusts is modified as

$$\omega^2 - \omega \omega_* - a \left( \omega_{pd+}^2 + \omega_{pd-}^2 \right) (1 - b A_{\pm}) = 0, \quad (14)$$

where  $\omega_* = -\frac{\left( \frac{\omega_{pd+}^2}{\Omega_{cd+}^2} + \frac{\omega_{pd-}^2}{\Omega_{cd-}^2} \right) \kappa_{ei} k_y}{k^2 + k_y^2 \left( \frac{\omega_{pd+}^2}{\Omega_{cd+}^2} + \frac{\omega_{pd-}^2}{\Omega_{cd-}^2} \right) + k_D^2}$  is the

dust drift frequency,  $A_{\pm} = \frac{(\dot{V}_{d+o} - \delta \dot{V}_{d-o})}{\Omega_{cd+}}$ ,  $k^2 =$

$k_y^2 + k_z^2$ ,  $a = \frac{k_z^2}{k^2 + k_y^2 \left( \frac{\omega_{pd+}^2}{\Omega_{cd+}^2} + \frac{\omega_{pd-}^2}{\Omega_{cd-}^2} \right) + k_D^2}$  and  $b =$

$\frac{k_y}{k_z} \left( \frac{\omega_{pd+}^2}{\omega_{pd+}^2 + \omega_{pd-}^2} \right)$ . The roots of (14) are

$$\omega = \frac{\omega_*}{2} \pm \frac{1}{2} \left[ \omega_*^2 + 4a \left( \omega_{pd+}^2 + \omega_{pd-}^2 \right) (1 - b A_{\pm}) \right]^{1/2} \quad (15)$$

Equation (15) with the  $+$  sign represents an accelerated mode and with the  $-$  sign it represents a retarded mode. Our interest is in the accelerated mode which shows an oscillatory instability for

$$\frac{\dot{V}_{d+0}}{\Omega_{cd+} \delta} > \left( \frac{\omega_*^2}{4ab \left( \omega_{pd+}^2 + \omega_{pd-}^2 \right) \delta} + \frac{1}{b\delta} + \frac{\dot{V}_{d-0}}{\Omega_{cd+}} \right).$$

For  $\dot{V}_{d-0} = \dot{V}_{d+0} = \dot{V}_o$  and  $\mu (= \frac{\dot{V}_o}{\Omega_{cd+}})$ , Eq. (15) is reduced to a new form

$$\omega = \frac{\omega_*}{2} \pm \frac{1}{2} \left[ \omega_*^2 + 4a \left( \omega_{pd+}^2 + \omega_{pd-}^2 \right) \{1 - b(1 - \delta)\mu\} \right]^{1/2}, \quad (16)$$

which is the dispersion relation for the coupled drift dust acoustic (CDDA) waves with sheared flows. The negative dust concentration and shear flow affect the frequency of the dust acoustic wave. Equation (15) exhibits an oscillatory instability of the CDDA wave if

$$\frac{\dot{V}_o}{\Omega_{cd+}} > \left( \frac{\omega_*^2}{4ab} + \frac{1}{b} + \frac{\delta \dot{V}_o}{\Omega_{cd+}} \right), \quad (17)$$

Furthermore, relation (17) can be written as

$$\frac{\dot{V}_o}{\Omega_{cd+}} > \frac{n_{eo} - n_{io}}{Z_{d+} n_{d+o}} \left( \frac{\omega_*^2}{4ab} + \frac{1}{b} \right),$$

which shows that negative dust particles play a stabilizing role in the instability and reduce the frequency of this electrostatic mode. For an inhomogeneous plasma, relation (15) will result in an unstable dust acoustic mode. This again shows that increasing the concentration of negative dust increases  $\delta$ , which decreases the instability which is exactly the same result as observed in [55]. For a homogeneous plasma and using the long wavelength approximation ( $\frac{k^2}{k_D^2} \ll 1$ ) relation (15) will become

$$\omega = \frac{c_{sd} k_z}{\sqrt{1 + \rho_{sd}^2 k_y^2}} \left( 1 - \frac{m_{d+}}{m_{d-}} \delta \frac{k_y}{k_z} A_{\pm} \right)^{1/2}$$

where  $c_{sd} = \sqrt{\frac{\omega_{pd+}^2 + \omega_{pd-}^2}{k_D^2}}$  is the dust acoustic speed due to both positive and negative dusts, while  $\rho_{sd} = \sqrt{\left( \frac{\omega_{pd+}^2}{\Omega_{cd+}^2} + \frac{\omega_{pd-}^2}{\Omega_{cd-}^2} \right) / k_D^2}$  is the dust gyro-radius impacted by the electron and ion temperatures. Instability of dust acoustic waves will occur if

$$A_{\pm} > \frac{m_{d-}}{m_{d+} \delta} \left( \frac{k_z}{k_y} \right).$$

## 4 Sheared Flow Driven Drift Vortices

We now discuss the quasi-stationary nonlinear solutions of the (6–7) as well as (10). In the quasi-stationary frame, we let  $\xi = y + \alpha z - ut$  where  $\alpha$  and  $u$  are constants giving the angle and speed of the nonlinear structures. Thus in the stationary frame (6) for positive and negative ions can be written as

$$D_{\xi\phi} v_{dj} z = -\frac{z_{dj} e}{m_{dj} u} (\mu_j \mp \alpha) \partial_{\xi} \phi \quad (18)$$

where  $D_{\xi\phi} = \left\{ \partial_{\xi} - \frac{c}{B_0 u} (\partial_x \phi \partial_{\xi} - \partial_{\xi} \phi \partial_x) \right\}$  and  $\mu_j (= \frac{\dot{V}_{dj} o}{\Omega_{cdj}})$ . Equation (18) shows that the accelerated mode will be unstable for  $\mu > \mu_c$  and stable for  $\mu < \mu_c$ , where it is obvious that for  $\mu \gg \mu_c$  the growth rate of instability reaches a maximum value which is roughly  $(ab)^{1/2} (n_{e0}/z_{d-} n_{d-0})^{1/2} (\mu)^{1/2} \omega_{pd+}$ . This means that the maximum growth rate of instability is directly proportional to the square root of  $\mu$  and the dust number density. It can be shown that (18) is exactly satisfied by

$$v_{dj} z = -\frac{z_{dj} e}{m_{dj} u} (\mu_j \mp \alpha) \phi, \quad (19)$$

Transforming (12) into the stationary frame and eliminating  $v_{dj} z$ , we obtain

$$D_{\xi\phi} (\nabla_{\perp}^2 \phi - \Gamma \phi) = 0, \quad (20)$$

$$\text{where } \Gamma = \frac{1}{\rho_{sd}^2} \left[ 1 - \frac{v_{*d}}{u} - \frac{c_{sd}^2 \alpha}{v_{*d}^2} \left( \alpha - \frac{\omega_{pd+}^2 A_{\pm}}{\omega_{pd+}^2 + \omega_{pd-}^2} \right) \right],$$

with  $v_{*d} = \frac{\kappa_{ei}}{k_D^2} \left( \frac{\omega_{pd+}^2}{\Omega_{cd+}} + \frac{\omega_{pd-}^2}{\Omega_{cd-}} \right)$  is being a modified drift speed. For the derivation of (20), it is assumed that  $\nabla_{\perp}^2 = \partial_x^2 + \partial_{\xi}^2 \gg \alpha^2 \partial_{\xi}^2$ . Equation (20) is a modified Hasegawa-Mima (HM) equation affected by the Boltzmann distributed electrons and ions as well as by dusts parallel sheared flows. The (20) analytically treats both a vortex street and a dipolar vortex solution, i.e., for  $\Gamma = 0$  and  $\Gamma \neq 0$  respectively, we will discuss these in turn.

### 4.1 Vortex Street Solution

In order to analytically determine the vortex street solution of (20), we substitute  $\Gamma = 0$ , so that (20) is satisfied by using a travelling like wave function

$$\nabla_{\perp}^2 \phi = \frac{L_1 L_2}{L_3} \exp \left[ -\frac{2}{L_1} \left( \phi - \frac{u B_0}{c} x \right) \right], \quad (21)$$

where  $L_1$  and  $L_2$  are arbitrary constants and  $L_3$  measures the size of the vortex street. The exact or analytical solution

of (21) is given by

$$\phi = \frac{u B_0}{c} x + L_1 \ln \left[ 2 \cosh (L_2 x) + 2 \left( 1 - L_3^{-2} \right) \cos (L_2 \xi) \right] \quad (22)$$

For  $L_3 > 0$ , the vortex profile given by (22) resembles the Kelvin-Stuart “cat’s eye” which represents a row of identical travelling vortices. The parameter  $L_1$  characterizes the amplitude of the vortex street. The vortex chain speed in the case of opposite dust is

$$u = \frac{v_{*d}}{2} \left[ 1 \pm \left\{ 1 - \frac{4c_{sd}^2 \alpha}{v_{*d}^2} \left( \alpha - \frac{\omega_{pd+}^2 A_{\pm}}{\omega_{pd+}^2 + \omega_{pd-}^2} \right) \right\}^{1/2} \right].$$

For  $L_3 = 1$ , Eq. (22) becomes a solution in the form of a zonal (a large scale) flow [32]

$$\phi = \frac{u B_0 x}{c} + L_1 \ln [2 \cosh (L_2 x)] \quad (23)$$

### 4.2 Double Vortex Solution

When  $\Gamma \neq 0$ , we get a double vortex solution and thus (20) is satisfied by the Ansatz

$$\nabla_{\perp}^2 \phi = C_1 \phi + C_2 x, \quad (24)$$

where  $C_1 (= \Gamma - \frac{c}{u B_0} C_2)$  and  $C_2$  are constants. To get the double vortex solution of (24), we transformed it to polar coordinates  $(r, \theta)$  such that  $x = r \cos \theta$ ,  $\xi = r \sin \theta$  where  $r = \sqrt{x^2 + \xi^2}$  and  $\theta = \tan^{-1}(\xi/x)$ . We divide the  $(r, \theta)$  plane into an outer region ( $r > R$ ) and an inner region ( $r < R$ ) of an arbitrary circle of radius  $R$ , called the vortex radius. In the outer region, to maintain boundedness of the solution, we must have  $C_2 = 0$  in order to avoid the direct dependence of the space variable  $x$ . Thus the solution of (24) for  $r > R$  becomes [56]

$$\phi_{\text{out}}(r, \theta) = Q_1 K_1 (\lambda_1 r) \cos \theta, \quad (25)$$

where  $Q_1$  is a constant,  $K_1$  is the first-order Mac-Donald function and  $\lambda_1 = \sqrt{\Gamma}$ . Since  $\lambda_1$  should be positive, for a well-behaved outer solution it is necessary that  $\Gamma$  should also be positive. Now for the inner region solution ( $r < R$ ), we have  $C_2 \neq 0$ , and assuming that  $\left( \Gamma - \frac{c}{u B_0} C_2 \right) = -\lambda_2^2$ , Eq. (24) then has homogeneous and nonhomogeneous parts. The homogeneous part becomes of the ordinary Bessel type and is treated as for the outer region. Thus the total solution for the inner region turns out to be

$$\phi_{\text{in}}(r, \theta) = \left( Q_2 J_1 (\lambda_2 r) + \frac{Q_3}{\lambda_2^2} r \right) \cos \theta, \quad (26)$$

where  $Q_3 = \frac{u B_0 (\lambda_1^2 + \lambda_2^2)}{c}$ ,  $Q_2$  and  $\lambda_2$  are constants and  $J_1$  is the Bessel function of order one. The constants of



integration  $Q_1$ ,  $Q_2$ , and  $\lambda_2$  can be found from the physically justified continuity conditions of  $\phi$ ,  $\partial_r \phi$ , and  $\nabla^2 \phi$  at the boundary of the circle, i.e., at  $r = R$ . For a given  $\lambda_1$ , the constant  $\lambda_2$  can be determined by using the transcendental equation  $\frac{K_2(\lambda_1 R)}{\lambda_1 K_1(\lambda_1 R)} = -\frac{J_2(\lambda_2 R)}{\lambda_2 J_1(\lambda_2 R)}$ , which may be obtained from continuation of  $\nabla_{\perp}^2 \phi$  at the vortex interface. Here,  $J_2$  and  $K_2$  are the Bessel and modified Bessel functions of the second order. The constants  $Q_1$  and  $Q_2$  are determined from the matching of electrostatic potential and electric field at the vortex interface and their respective values are

$$Q_1 = \frac{u B_o}{c} \frac{R}{K_1(\lambda_1 R)},$$

$$Q_2 = -\frac{u B_o}{c} \frac{\lambda_1^2}{\lambda_2^2} \frac{R}{J_1(\lambda_2 R)}.$$

## 5 Results and Discussion

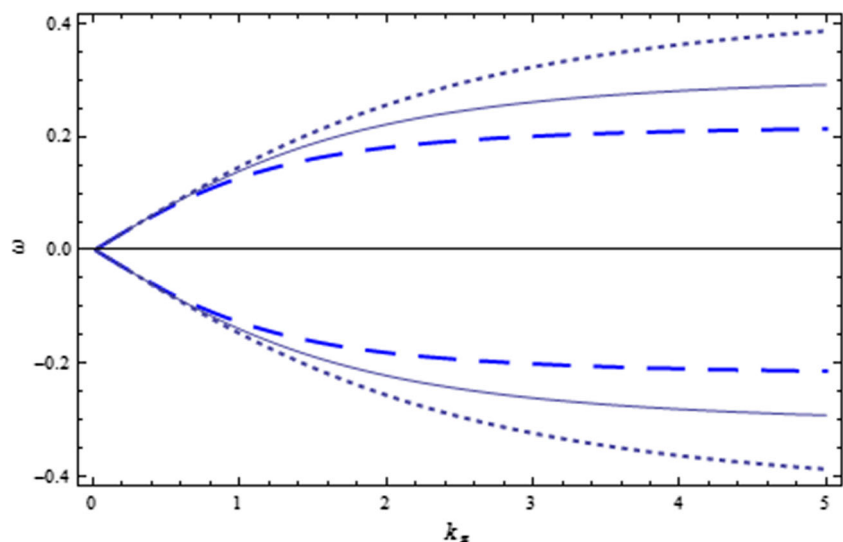
We have plotted the dispersion relations by using some typical parameters of four component dusty plasmas, as used in laboratory plasmas [57], as  $T_e = 0.08$  eV,  $T_i = 0.5 T_e$ ,  $B_0 = 0.3$  T,  $n_{d-o} = 10^6/\text{cm}^3$ ,  $n_{d+o} = 0.7 n_{d-o}$ ,  $n_{e0} = 0.2 n_{d-o}$ ,  $n_{i0} = 0.5 n_{d-o}$ ,  $k_y \sim \text{few centimeter}$ , let it be  $\simeq 10$  cm,  $m_{d+} \sim 2 \times 10^{-18}$  kg,  $m_{d-} \sim 2.3 \times 10^{-18}$  kg,  $Z_{d+} = 5$ ,  $Z_{d-} = 6$ ,  $\kappa_{ei} = -0.005$  and  $\left| \frac{\hat{V}_{d\pm 0}}{\Omega_{cd\pm}} \right| \sim 0.4$ . The graphical analysis of the two modes of relation (15) are presented in Figs. 1 and 2 by using the above mentioned numerics for coupled drift-dust-acoustic (DDA) waves with populations of opposite polarity and sheared flow of negative and positive dusts. Figure 1 shows the signification of dust number density on the wave frequency against the parallel wave

number  $k_z$  for fixed perpendicular wave number  $k_y$ . The condition  $k_z < k_y$  is employed here to plot the dispersion relation. It is obvious from Fig. 1 that  $\omega$  of the forward and backward propagating DDA waves is increasing with increased values of negative dust number density  $n_{d-o}$ . It means that most of the dynamical role to drive the coupled drift-dust acoustic waves is carried out by the negative dust particles. Thus negative dust steadies the DDA mode contrary to positive dust, which enhances the instability in the system and as a result the DDA waves grow exponentially, extracting energy from the equilibrium density gradient and starting interactions with each other.

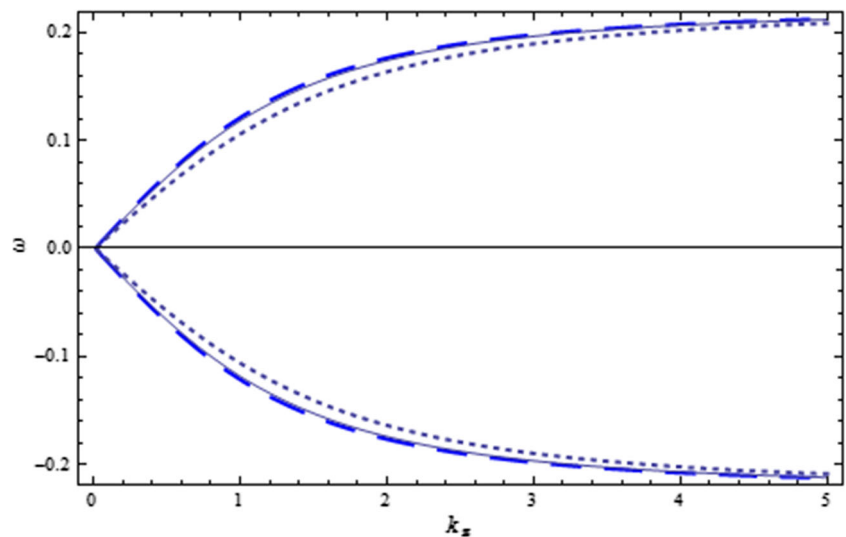
The plots of the frequency  $\omega$  as a function of  $k_z$  for both forward and backward propagating DDA modes are shown in Fig. 2, for three values of ion temperature. The plots show an increasing trend with respect to  $k_z$ , and for increased values of  $T_i$  the frequency  $\omega$  increases with respect to  $k_z$ . Temperature effects of both ions and electrons show that for DDA mode these temperatures play a vital role in compression and rarefaction of both positive and negative dusts. It signifies that the acoustic mode in such a four component plasma is being changed in character because of electrons and ions temperature.

We now parametrically investigate the effects of sheared flow and dust polarity on the behavior of DDA mode by employing the above-mentioned parameters by using a 3D plot in Fig. 3. The plot shows that frequency  $\omega$  decreases with increased values of both sheared flow  $\frac{\hat{V}_{d\pm 0}}{\Omega_{cd\pm}}$  and  $k_y$ . Thus the effect of the sheared flow is such that it affects the dynamics of DDA modes and can distort the structure, and at large values there is a possibility that it will lead to collapse these mode structures. We conclude that solutions of DDA modes in the presence of sheared flow can be attained under certain prevailing assumptions, and beyond

**Fig. 1** The frequency of the drift-dust-acoustic wave  $\omega$  against  $k_z$  with the effect of negative dust number density  $n_{d-o}$ , such that  $n_{d-o} = 10^6$  (dashed line)  $2 \times 10^6$  (solid line) and  $4 \times 10^6$  (dotted line). The wave number  $k_z$  is scaled to  $k_z/10^{-3}$  and frequency  $\omega$  is  $\omega/10^4$ . All other parameters are the same as mentioned in Section 5



**Fig. 2** The frequency of the drift-dust-acoustic wave  $\omega$  against  $k_z$  with the effect of the ratio of ion to electron temperature, such that  $\frac{T_i}{T_e} = 0.5$  (dashed line),  $\frac{T_i}{T_e} = 0.3$  (solid line), and  $\frac{T_i}{T_e} = 0.1$  (dotted line). The wave number  $k_z$  is scaled to  $k_z/10^{-3}$  and frequency  $\omega$  is  $\omega/10^4$ . All other parameters are the same as mentioned in Section 5



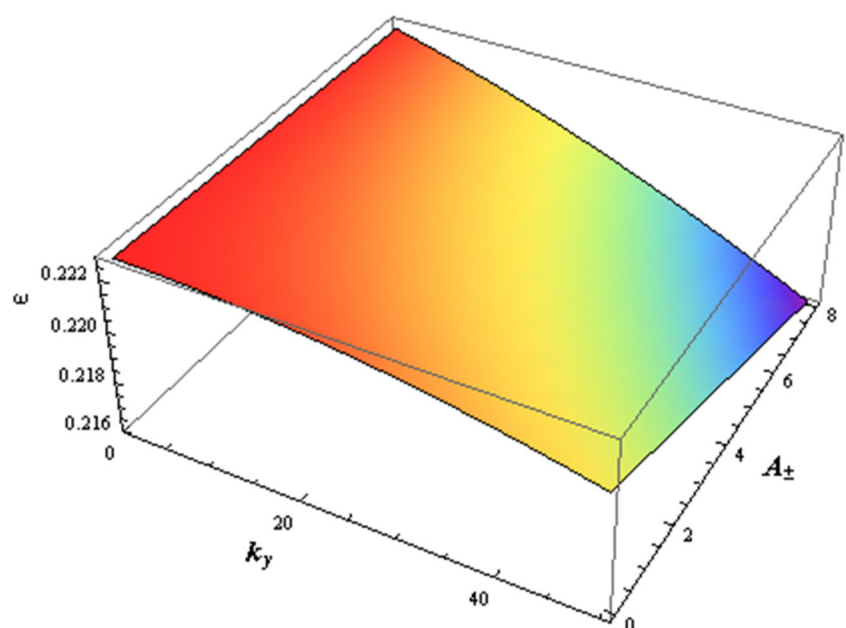
those assumptions there is a possibility that these modes will not exist.

Figure 4 shows the contour plots in the  $(x, \xi)$  plane, which are based on (24) and (25) by utilizing the above data. It shows that for positive values of  $x$  the electrostatic potential shows a “hill,” with the values of the contour increasing equally from 0.12 to 1. For negative values of  $x$ , a “well,” structure is observed, with the values of the contour decreasing from  $-0.12$  to  $-1$ . Since the drift velocity is defined by  $1/B_0 \hat{z} \times \nabla \phi$ , the fluid velocity shows a clockwise behavior for the positive  $x$  (i.e., potential hill) and counterclockwise nature for the negative  $x$  values (i.e., potential well). The nonlinear drift and acoustic dipolar vortex structures are

formed on spatial scale lengths of the order of  $\rho_{sd}$ , which is an effective Larmor radius due to both positive and negative dusts.

To summarize, we have investigated both the linear and nonlinear properties of low-frequency electrostatic waves containing equilibrium density gradient and plasma flow inhomogeneities in a nonuniform four components dusty plasma. Our analysis has shown that free energy stored in the sheared flow can be coupled with dust drift and dust acoustic waves. It is also shown that positive and negative sheared flow in a plasma can produce an instability. The differential flow gradient can be caused because of an inhomogeneity in the density gradient. This type of instability

**Fig. 3** Bird's eye view of the effect of sheared flow  $A_{\pm}$  on the frequency of the drift-dust-acoustic wave  $\omega$  as a function of  $k_y$  for fixed value of  $k_z \sim 10$ . All other parameters are the same as mentioned in Section 5





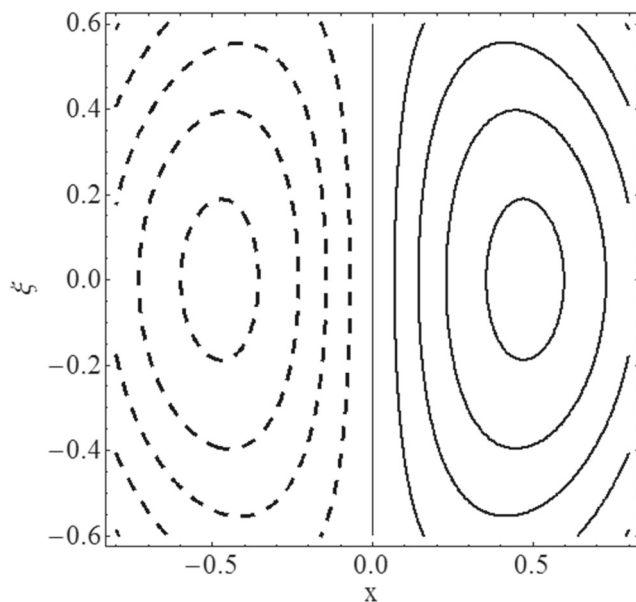


**Fig. 4** The contour plots of the electrostatic potential  $\phi$  corresponding to solutions of (24) and (25) are plotted in the  $(x, \xi)$  plane by choosing some typical parameters as given in the text. For positive values of  $x$ , the electrostatic potential shows a “hill,” with the values of the contour increasing evenly from 0.12 to 1. For negative values of  $x$ , a “well” structure is observed, with the values of the contour decreasing from  $-0.12$  to  $-1$

has the same mechanism as the Kelvin-Helmholtz instability, where the inhomogeneous flow among the consecutive layers has invoked a slippage mechanism. In the linear portion, we have derived a new type of dispersion relation, which shows the dependence of the frequencies of forward and backward propagating DDA waves on dust density as well as ion and electron temperatures. In the nonlinear part, the sheared plasma flow and inhomogeneity in density causes the electrostatic perturbations to interact and transfer their free energy within the wave spectra. In this case, the drift-acoustic modes interact with convective cells. This coupling causes a self-organized state in which vorticity is formed in either Kelvin-Stuart “cat’s eyes” type solutions, which are chain vortices, or admits to a double vortex solution. These convective non-linear vortical structures are caused by mode coupling equations which contain vector nonlinearity. The speed of the vortices strongly depends on different equilibrium plasma parameters such as density, temperature, and magnetic fields. The solutions of these turbulences are always obtained in the form of vortex street and double vortices. Our approach in this opposite dust polarity work is more analytical, but these analytical results should be useful in understanding the physical wave phenomena and associated nonlinear structures in space and laboratory plasma in the presence of Boltzmann electrons and ions.

## References

1. M. Horanyi, *Annu. Rev. Astron. Astrophys.* **34**, 383 (1996)
2. D.A. Mendis, M. Horanyi, in *Cometary Plasma Processes, Monograph 61* ed. by A. D. Johnstone (American Geophysical Union, Washington, 1991), pp. 17–25
3. O. Havnes, J. Trøim, T. Blix, W. Mortensen, L.I. Næsheim, E. Thrane, T. Tønnesen, *J. Geophys. Res.* **101**, 10839 (1996)
4. M. Horanyi, G.E. Morfill, E. Grün, *Nature (London)* **363**, 144 (1993)
5. P.K. Shukla, A.A. Mamun, *Introduction to Dusty Plasma Physics*, (Institute of Physics, Bristol, 2002)
6. N.N. Rao, P.K. Shukla, M.Y. Yu, *Planet. Space Sci.* **38**, 543 (1990)
7. A. Barkan, R.L. Merlino, N. D’Angelo, *Phys. Plasmas* **2**, 3563 (1995)
8. P.K. Shukla, V.P. Silin, *Phys. Scr.* **45**, 508 (1992)
9. A. Barkan, N. D’Angelo, R.L. Merlino, *Planet. Space Sci.* **44**, 239 (1996)
10. V.E. Fortov, A.P. Nefedov, O.S. Vaulina, A.M. Lipaev, V.I. Molotokov, A.A. Samarian, V.P. Nikitskii, A.I. Ivanov, S.F. Savin, A.V. Kalmykov, A.Ya. Solov’ev, P.V. Vinogradov, *J. Exp. Theor. Phys.* **87**, 1087 (1998)
11. V.W. Chow, D.A. Mendis, M. Rosenberg, *J. Geophys. Res.* **98**, 19065 (1993)
12. M. Rosenberg, D.A. Mendis, D.P. Sheehan, *IEEE Trans. Plasma Sci.* **27**, 239 (1999)
13. T.A. Ellis, J.S. Neff, *Icarus* **91**, 280 (1991)
14. P.K. Shukla, M. Rosenberg, *Phys. Scr.* **73**, 196 (2006)
15. D.J. Lacks, A. Levandovsky, *J. Electrostat.* **65**, 107 (2007)
16. G.D. Freier, *J. Geophys. Res.* **65**, 3504 (1960)
17. J. Merrison, J. Jensen, K. Kinch, R. Mugfor, P. Nornberg, *Planet. Space Sci.* **52**, 279 (2004)
18. C.D. Stow, *Rep. Prog. Phys.* **32**, 1 (1969)
19. H. Zhao, G.S.P. Castle, I.I. Inculet, *J. Electrostat.* **55**, 261 (2002)
20. H. Zhao, G.S.P. Castle, I.I. Inculet, A.G. Bailey, *IEEE Trans. Ind. Appl.* **39**, 612 (2003)
21. S. Trigwell, N. Grable, C.U. Yurreri, R. Sharma, M.K. Mazumder, *IEEE Trans. Ind. Appl.* **39**, 79 (2003)
22. F. Sharmene Ali, M. Adnan Ali, R. Ayesha Ali, I.I. Inculet, *J. Electrostat.* **45**, 139 (1998)
23. D.A. Mendis, M. Rosenberg, *Ann. Rev. Astron. Astrophys.* **32**, 419 (1994)
24. A.A. Mamun, P.K. Shukla, *Geophys. Res. Lett.* **29**, 1870 (2002)
25. A.A. Mamun, *Phys. Rev. E* **77**, 026406 (2008)
26. A.A. Mamun, *Phys. Lett. A* **372**, 686 (2008)
27. A. Saha, P. Chatterjee, *Braz. J. Phys.* **45**, 419 (2015)
28. A. Saha, P. Chatterjee, N. Pal, *J. Plasma Phys.* **81**, 905810509 (2015)
29. A. Saha, P. Chatterjee, *Astrophys. Space Sci.* **351**, 533 (2014)
30. A. Saha, P. Chatterjee, *Phys. Plasmas* **21**, 022111 (2014)
31. G. Mandal, K. Roy, A. Paul, A. Saha, P. Chatterjee, *Z. Naturforsch.* **70**(9a), 703 (2015)
32. P.K. Shukla, T. Farid, L. Stenflo, O.G. Onishchenko, *J. Plasma Phys.* **64**, 427 (2000)
33. A.M. Mirza, T. Farid, P.K. Shukla, L. Stenflo, *IEEE Trans. Plasma Sci.* **29**, 298 (2001)
34. Q. Haque, H. Saleem, A.M. Mirza, *Phys. Plasmas* **12**, 104504 (2005)
35. J. Vranjes, S. Poedts, *Plasma Sources Sci. Technol.* **14**, 485 (2005)
36. M.E. Koepke, J.J. Carroll, M.W. Zintl, *J. Geophys. Res.* **104**, 14397 (1999)
37. M.E. Koepke, *Phys. Plasmas* **9**, 2420 (2002)
38. N. D’Angelo, A. Bahnsen, H. Rosenbauer, *J. Geophys. Res.* **79**, 3129 (1974)
39. M.C. Kelley, C.W. Carlson, *J. Geophys. Res.* **82**, 2344 (1977)

40. A.W. Yau, B.A. Whalen, A.G. McNamara, P.J. Kellogg, W. Bernstein, J. Geophys. Res. **88**, 341 (1983)
41. Su. Basu, J. Geophys. Res. **93**, 115 (1988)
42. Ö. Kivanc, R.A. Heelis, Geophys. Res. Lett. **26**, 1829 (1999)
43. G.D. Earle, M.C. Kelley, G. Ganguli, J. Geophys. Res. **94**, 15321 (1989)
44. G. Ganguli, M.J. Keskinen, H. Romero, R. Heelis, T. Moore, C. Pollock, J. Geophys. Res. **99**, 8873 (1994)
45. E. Agrimson, N. D'Angelo, R.L. Merlino, Phys. Rev. Lett. **86**, 5282 (2001)
46. E. Agrimson, N. D'Angelo, R.L. Merlino, Phys. Lett. A **293**, 260 (2002)
47. C. Teodorescu, E.W. Reynolds, M.E. Koepke, Phys. Rev. Lett. **88**, 185003 (2002)
48. D.L. Jassby, Rev. Sci. Instrum. **42**, 1355 (1971)
49. M. Yamada, D.K. Owens, Phys. Rev. Lett. **38**, 1529 (1977)
50. W.E. Amatucci, G. Ganguli, D.N. Walker, G. Gatling, M. Balkey, T. McCulloch, Phys. Plasmas **10**, 1963 (2003)
51. E. Thomas, J.D. Jackson, E.A. Wallace, G. Ganguli, Phys. Plasmas **10**, 1191 (2003)
52. N. Sato, M. Nakamura, R. Hatakeyama, Phys. Rev. Lett. **57**, 1227 (1986)
53. Q. Haque, W. Masood, H. Saleem, Phys. Scr. **77**, 035502 (2008)
54. D. Jovanovic, P.K. Shukla, Phys. Plasmas **6**, 976 (1999)
55. R. Ichiki, T. Kaneko, K. Hayashi, S. Tamura, R. Hatakeyama, Plasma Phys. Control. Fusion **51**, 035011 (2009)
56. J. Liu, W. Horton, J. Plasma Phys. **36**, 1 (1986)
57. N. D'Angelo, Planet. Space Sci. **49**, 1251 (2001)